



University of
New Haven

University of New Haven
Digital Commons @ New Haven

Civil Engineering Faculty Publications

Civil Engineering

12-2018

Degradation of 3-Nitro-1, 2, 4-Trizole-5-One (NTO) in Wastewater with UV/H₂O₂ Oxidation

Amalia Terracciano

Stevens Institute of Technology

Christos Christodoulatos

Stevens Institute of Technology

Agamemnon Koutsospyros

University of New Haven, akoutsospyros@newhaven.edu

Zhaoyu Zheng

Stevens Institute of Technology

Tsan-Liang Su

Stevens Institute of Technology

See next page for additional authors

Follow this and additional works at: <https://digitalcommons.newhaven.edu/civilengineering-facpubs>

 Part of the [Civil Engineering Commons](#)

Publisher Citation

Terracciano, Amalia, Christos Christodoulatos, Agamemnon Koutsospyros, Zhaoyu Zheng, Tsan-Liang Su, Benjamin Smolinski, Per Arienti, and Xiaoguang Meng. "Degradation of 3-nitro-1, 2, 4-trizole-5-one (NTO) in wastewater with UV/H₂O₂ oxidation." *Chemical Engineering Journal* 354 (2018): 481-491.

Comments

This is the authors' accepted version of the article published in *Chemical Engineering Journal*. The published version can be accessed at <https://doi.org/10.1016/j.cej.2018.07.216>.

Authors

Amalia Terracciano, Christos Christodoulatos, Agamemnon Koutsospyros, Zhaoyu Zheng, Tsan-Liang Su, Benjamin Smolinski, Per Arienti, and Xiaoguang Meng

Degradation of 3-nitro-1, 2, 4-triazole-5-one (NTO)

In wastewater with UV/H₂O₂ oxidation

Amalia Terracciano^a, Christos Christodoulatos^a, Agamemnon Koutsospyros^b, Zhaoyu Zheng^c, Tsan-Liang Su^a, Benjamin Smolinski^d, Per Arienti^d and Xiaoguang Meng^{a*}

^aCenter for Environmental Systems,

Stevens Institute of Technology, Hoboken, NJ 07030, USA

^bUniversity of New Haven, West Haven, CT 06156, USA

^cCenter for Mass Spectrometry,

Stevens Institute of Technology, Hoboken, NJ 07030, USA

^dUS Army RDECOM-ARDEC, Picatinny, NJ 07806-5000, USA

*corresponding author. tel: +1 201 2168014; fax: +1 201 2168303

e-mail: xmeng@stevens.edu

Abstract

Insensitive Munition (IM) formulations contain 3-nitro-1,2,4-triazole-5-one (NTO), an energetic compound with the highest aqueous solubility (16 g L^{-1}) among all IM explosives, including 2, 4-dinitroanisole (DNAN) and 1-nitroguanidine (NQ); as a result wastewater streams from IM processing facilities can be highly contaminated and potentially toxic. The removal of energetic compounds from wastewater streams prior to their discharge in the environment is imperative, and new technology must be developed to efficiently treat high levels of NTO and other IM compounds in these streams. In this study, the treatment of NTO wastewater by a UV/H₂O₂ oxidation process under acidic conditions ($\text{pH} = 3.0 \pm 0.1$) and a hydrogen peroxide concentration of at least 1500 mg L^{-1} resulted in successful removal of the energetic compound. The organic carbon from the NTO ring was completely converted to inorganic carbon (CO₂), as confirmed through TOC measurements and GC-MS analysis on the reactor headspace. Nitrate and ammonium ions were the major nitrogen by-products, as indicated by mass spectrometry. The results obtained in this work demonstrate that the UV/H₂O₂ oxidation process can effectively mineralize high concentrations of NTO in wastewater streams leading to recovery of valuable nutrients that can be used for supporting algal biomass growth for biofuel/biogas generation.

Keywords

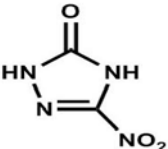
NTO, UV/H₂O₂, oxidation, mineralization, pH and H₂O₂ effects, MS

1. Introduction

In the last decade, defense programs have invested significant time and effort into developing safer, insensitive munitions (IM) which will be less sensitive to shock and chemically more stable [1]. In fact, the conventional munitions components, such as hexahydro-1, 3, 5-triazacyclohexane (RDX, $C_3H_6N_6O_6$), octahydro-1, 3, 5, 7-tetrazocine (HMX, $C_4H_8N_8O_8$) and especially the more classic 2, 4, 6-trinitrotoluene (TNT, $C_7H_5N_3O_6$), have been often associated with accidental explosions [2,3] in addition to their toxicity and mutagenicity characteristics [4,5].

More recently, the insensitive munition formulation IMX-101 has been developed and approved for replacement of TNT in most munitions [6]; the main ingredients used in the IMX-101 formulation are 2, 4-dinitroanisole (DNAN, $C_7H_6N_2O_5$), 3-nitro-1, 2, 4-triazole-5-one (NTO, $C_2H_2N_4O_3$) and 1-nitroguanidine or picrite (NQ, $CH_4N_4O_2$). NTO (Table 1) in particular has attracted significant interest since it exhibits energetic performance similar to RDX but with much higher stability against constraints such as pressure, heat, impact and friction [7].

Table 1. Chemical characteristics and structure of NTO [9].

Structure	Molecular weight (g mol ⁻¹)	Density (g cm ⁻³)	Flash Point (C°)	Boiling point at 1 atm (C°)	Solubility at 25 C° (mg L ⁻¹)
	130.063	2.4±0.1	103.5±22.6	247.5±23.0	16,000

Because of the growing applications of DNAN, NQ and NTO in the production of IMX-101, manufacturing facilities generate large volumes of explosive-laden wastewater from cleaning and repacking operations, which require cost-effective remediation processes. NTO has the highest solubility (12.8 g L⁻¹ at 20 C° and 16 g L⁻¹ 25 C° [8, 9]) among the IM constituents, making it easily dissolved in water under typical environmental conditions, which could result in human

exposure to the chemical. While NTO showed low toxicity toward freshwater organisms [10, 11], it is a male reproductive toxicant in rats [12] and was reported to form transformation products that can be toxic [13]. Based on this scenario, the investigation of suitable technologies for treatment of NTO-contaminated wastewater is a topic of particular concern.

Microbial degradation of the IMX-101 components under both oxic and anoxic conditions has been reported in several studies [13,14,15]; however, biodegradation required up to two weeks in order to obtain complete mineralization of NTO and only low concentrations ($<50 \text{ mg L}^{-1}$) could be treated [15]. The energetic-laden wastewaters contain high concentrations of NTO, which require treatment capable of degrading the energetic compound at high efficiency. In addition to removal and detoxification, it is a renovated interest the application of treatments techniques that can convert wastewater streams into media for cultivating microalga biomass, which can be used for energy recovery in the form of biofuel and/or biogas [16].

Advanced Oxidation Processes (AOPs) have found extensive application in treatment of industrial wastewaters due to their lower environmental impact than alternative technologies. In fact, AOPs neither transfer pollutants from one phase to the other nor produce significant amounts of hazardous sludge but oxidize and mineralize the target contaminants to stable inorganic and ionic species. The successful application of AOPs in treatment of RDX, HMX and TNT has been already documented in several studies [17, 18, 19]. In particular, ultraviolet photolysis in combination with hydrogen peroxide oxidation (UV/H₂O₂) is one of the most common and efficient AOP techniques applied. This process involves the photolysis of hydrogen peroxide to generate hydroxyl radicals ($\cdot\text{OH}$), which attack the target organic compounds with rate constants ranging from 10^6 to $10^{10} \text{ M}^{-1} \text{ s}^{-1}$ [20], oxidizing them by hydrogen atom abstraction or by addition to double bonds [21]. Specifically, the UV/H₂O₂ technique has been successfully used for the

destruction of chlorophenols and other chlorinated compounds [22, 23] as well as the mineralization of atrazine, desethylatrazine, simazine [24] and nitroaromatic compounds [25].

At present, only one study has been reported on the application of AOPs to NTO-contaminated wastewater, which showed that the photodegradation of NTO with the UV/H₂O₂ method occurs only in the presence of titanium dioxide (TiO₂) as a catalyst [26].

In this work, UV/H₂O₂ oxidation was applied to the treatment of both synthetic and industrial NTO wastewater with energetic compound concentration as high as 8.4 g L⁻¹ (65 mmol L⁻¹). The degradation process was characterized extensively through kinetic tests under different conditions (NTO, H₂O₂ concentration and pH) and optimal parameters for the removal process were determined; the organic carbon and nitrogen by-products from the chemical degradation of NTO were also identified and quantified. The major intent of this study is to provide new information on the application of UV/H₂O₂ oxidation to the treatment of wastewater streams contaminated with NTO.

2. Materials and methods

2.1. Chemicals and experimental set-up

All chemicals used were ACS grade purchased from Fisher Scientific (Pittsburg, PA). Kinetic experiments were performed on both synthetic and industry-generated NTO wastewater; the synthetic NTO wastewater was obtained by dissolving pure NTO powder in deionized (DI) water while the NTO-contaminated wastewater was provided from a munitions production facility. For each experiment, 800 ml of NTO wastewater/solution was placed in a 1000 ml volume (H=19 cm; d(in)=8.5 cm) glass beaker (Corning Pyrex glass beaker, Fisher Scientific, Pittsburgh, PA) set on a mixer with magnetic bar stirring. The UV light used for the tests was provided by a UV low-pressure discharge lamp which emitted at 254 nm wavelength (LSE Lighting UV bulbs, UV-C,

germicidal type, 13 W); the lamp, protected by a quartz glass sleeve, was placed directly into the solution/wastewater at a depth of 15 cm, resulting in a contact area of 113 cm². The fluence rate or irradiance (mW cm⁻²) delivered by the lamp was continuously monitored beforehand in a blank system (DI water) over a time period of 24 hours; a lamp irradiance of 8.5±0.5 mW cm⁻² was found to be constant over the observed time, as shown in Fig. S1.

A pre-fixed amount of H₂O₂ was added to the prepared solution/wastewater (reagent grade hydrogen peroxide, 34-37%, Fisher Scientific, Pittsburgh, PA) and the reaction was initiated by switching the UV light on. The treatment apparatus and UV lamp bulbs were placed in a dark chamber to ensure no contact with other artificial/natural light sources during the treatment time.

A gas-tight reactor of 1000 ml volume was used for determination of the gaseous end products from oxidation of NTO; for this purpose, GC-MS analyses were performed on gaseous samples collected from the headspace of the reactor at different time intervals.

2.2. NTO wastewater characterization

A summary of the physical and chemical characteristics of the industry-generated wastewater used is reported in Table 2. The wastewater had a high concentration of NTO (8.4 g L⁻¹; 65 mmol L⁻¹), high pH (12±0.1), high total alkalinity (22 g L⁻¹ as CaCO₃), and a dark orange/red color (Fig. S2) which resulted in significant turbidity (1.84±0.5 NTU). The NTO wastewater had noticeably different characteristics from the synthetic NTO solution (Table 2), which is probably due to the industrial processing used in the plant production line. In particular, for the same NTO concentration (8.0 g L⁻¹; 62 mmol L⁻¹) the synthetic wastewater acquired a light yellow color and acidic pH (3.2±0.1). The absorption spectra of the synthetic NTO solution and NTO wastewater in the wavelength range 200-700 nm also showed some differences, even though both spectra exhibited high absorbance in the range 250-350 nm (Fig.S3).

The carbon (NTO-[C]) and nitrogen (NTO-[N]) concentrations associated with NTO wastewater (8.4 g L^{-1}); were calculated as 1567 mg-C L^{-1} ($131 \text{ mmol-C L}^{-1}$) and 3656 mg-N L^{-1} ($261 \text{ mmol-N L}^{-1}$). However, in the industrial wastewater the measured total nitrogen (TN-M) was higher than the nitrogen calculated from NTO ($5928 \text{ mg-N L}^{-1} > 3656 \text{ mg-N L}^{-1}$), indicating that other species, such as nitrite (NO_2^-) and nitrate (NO_3^-) ions (Table 2), contributed to the total nitrogen balance in the wastewater. Mass Spectrometry (MS) analysis of the raw wastewater did not detect any other organic compounds besides NTO, which is consistent with the calculated (NTO-[C]) and measured total organic carbon concentrations (TOC). The two strong peaks found at m/z 129 and m/z 62 correspond to $[\text{NTO-H}]^-$ ion and NO_3^- respectively (Fig. 1). NTO was detected in the form of $[\text{NTO-H}]^-$ ion, as under negative-ion-generating conditions NTO loses a proton, which results in a peak at m/z 129; the peaks at m/z 147 and m/z 214 were attributed to $[\text{NaNO}_3 \cdot \text{NO}_3]^-$ and $[\text{NaNO}_3 \cdot \text{NTO-H}]^-$ complexes, while the peak at m/z 45 represents a blank peak.

Toxicological tests on the NTO wastewater conducted with freshwater green microalgae *Scenedesmus obliquus* (ATCC ® 11477TM) showed high inhibition on growth of the microalgae (Fig S4a) which is indication of significant toxicity. A lower inhibition was exhibited for the diluted NTO wastewater (2x dilution, $\text{NTO(w)} = 4200 \text{ mg L}^{-1}$, 37.3 mmol L^{-1}) but only up to 10% of the sample (Fig.S4b).

Table 2. Physical chemical characteristics of NTO wastewater and NTO synthetic solution.

NTO	pH	Turbidity (NTU)	NTO (mg L^{-1})	TOC (mgC L^{-1})	$\text{NO}_2\text{-N}$ (mgN L^{-1})	$\text{NO}_3\text{-N}$ (mgN L^{-1})	$\text{NH}_4\text{-N}$ (mgN L^{-1})	Total N (mgN L^{-1})
Waste water	12 ± 0.1	1.84 ± 0.5	8451 ± 50	1559 ± 50	735.5 ± 10	2881 ± 15	5.853 ± 0.6	5928 ± 80
synthetic	3.2 ± 0.1	0.35 ± 0.5	8000 ± 10	1422 ± 5.0	0.352 ± 0.05	35.90 ± 2.0	0.545 ± 0.05	3450 ± 10

2.3. Analytical Methods

MS analysis of the liquid samples from NTO wastewater/solution, prior and post treatment, was conducted with a triple-quadrupole tandem mass spectrometer (Quattro Ultima, Waters, Milford, MA) equipped with an electrospray ion source, using N₂ as the nebulizer and desolvation gas, under negative-ion-generating conditions. NTO wastewater/solution was infused into the source by a syringe pump at a flow rate of 20 $\mu\text{L} \cdot \text{min}^{-1}$ through a stainless-steel capillary (I.D. 0.1 mm) which was held at a voltage of 3.0 kV. The source temperature was held at 100 °C, and the desolvation gas temperature was held at 150 °C. All the mass spectra were recorded over a range of m/z from 10 to 500 with a unit mass resolution (peak width at half height) of approximately 0.6 Da.

GC-MS measurements on headspace gaseous samples were performed with a Hewlett-Packard 6890 series GC system coupled with a Hewlett-Packard 5973 mass selective detector. An Agilent DB-1 column (30 m \times 250 μm id, 1.00 μm) was used for the separation with Helium as carrier gas and a flow rate of 0.7 mL/min. For each analysis, 10 μL of sample was manually injected in the inlet, which was kept at 250 °C; analysis was carried out in split mode (20:1) with a set temperature program (oven temperature held at 40 °C for 0.5 min, then increased to 150 °C at a rate of 20 °C /min). The MS transfer line temperature was 220 °C, while the mass selective detector was held at 230 °C, with detection mass range m/z from 10 to 100.

FTIR measurements of the NTO wastewater were performed using a Thermo-Nicolet Nexus IS50 spectrometer equipped with a horizontal attenuated total reflectance (HATR) cell (PIKE Tech) and a liquid-nitrogen-cooled mercury-cadmium-telluride (MCT) detector. A multibounce ZnGe IR crystal with 45° beveled faces (infrared angle of incidence, θ) was used, and the infrared spectra were collected using 512 scans per spectrum at a resolution of 4 cm^{-1} . A

background spectrum consisting of the absorbance of the ZnSe crystal and DI water was collected before sample measurements.

NTO concentrations were analyzed by high-performance liquid chromatography (HPLC) using an Agilent, Infinity Series, 1260 system equipped with a DAD detector. A porous graphitic carbon (PGC) Hypercarb column (Thermo Scientific, Waltham, MA) with guard column (C-18, 5- μ m, Alitech, Deerfield, IL) was used for the separation. NTO was quantified using an isocratic mobile phase 70:30 by volume consisting of water and acetonitrile with 0.1% TFAA (HPLC grade chemicals, Fisher Scientific, Pittsburgh, PA) at a flow rate of 1.0 mL min⁻¹ and detector wavelength at 254 nm (M.D.L. 0.1 mg L⁻¹). All samples were filtered using 0.45 μ m pore size syringe filters (Fisher Brand, Waltham, MA) prior to HPLC analysis.

The total nitrogen (TN), nitrite (NO₂⁻) and ammonium (NH₄⁺) concentrations were analyzed using an ultraviolet spectrophotometer (DR6000, HACH, Loveland, CO) with dedicated test kits for nitrogen compound analysis (D.L. TN=5 mg L⁻¹; NO₂⁻=0.005 mg L⁻¹; NH₄⁺= 0.1 mg L⁻¹). Nitrate (NO₃⁻) concentrations were analyzed using an ion chromatograph (IC) with IonPac®AS11 (4 mm×250 mm, DIONEX, Thermo Scientific, Waltham, MA), equipped with a guard column (IonPac®AG16 (4 mm×50 mm) DIONEX, Thermo Scientific, Waltham, MA). The mobile phase consisted of 12 mM KOH solution in DI water with an eluent flow rate of 1 ml min⁻¹ (M.D.L. 0.1 mg L⁻¹).

Hydrogen peroxide (H₂O₂) concentrations were measured using a dedicated test kit (Model HYP-1, HACH, Loveland, CO) and a titration method by addition of Thiosulfate reagent (D.L. 1.0 mg L⁻¹).

The total alkalinity of the NTO wastewater was measured using acid titration with H_2SO_4 according to the standard procedure reported in “Standard Methods for the Examination of Water and Wastewater” (E.P.A., Method 2320B).

Total organic carbon (TOC) concentrations were analyzed using a Phoenix 8000 UV-Persulfate TOC analyzer (Teledyne Tekmar Company, Mason, OH), equipped with a TOC boat sampler (Rosemount Dohrmann Model 183, Teledyne Tekmar Company, Mason, OH), and TOC Talk software (Teledyne Tekmar Company, Mason, OH) (M.D.L. 0.5 mg L^{-1}). The instrument was calibrated each time with a set of TOC standards prepared by dilution of a 1000 mg-C L^{-1} stock solution (SCP Science, Champlain, NY) with DI water (Nanopure infinity system, Barnstead, Dubuque, IA, at $>18.2 \text{ M}\Omega \text{ cm}$ at 25°C).

The UV irradiance or fluence rate (mW cm^{-2}) was monitored with a UV-C digital Light meter (HHUV254sd, Omega) ($2\text{-}20\pm4\%$ full scale range, mW cm^{-2}) by placing the UV-C probe directly into the solution at a fixed distance of 1 cm from the light source.

Toxicity tests were performed as described in the OECD Guidelines (2011). The procedure was adapted to 24 well-microplates using the commercial medium BG-11 (composition: $1,500 \text{ mg NaNO}_3$, 75 mg MgSO_4 , $40 \text{ mg K}_2\text{HPO}_4$, $36 \text{ mg CaCl}_2 \cdot 2\text{H}_2\text{O}$, $20 \text{ mg Na}_2\text{CO}_3$, 6 mg citric acid (vitamin C), 6 mg ferric ammonium citrate, $2.86 \text{ mg H}_3\text{BO}_3$, $1.81 \text{ mg MnCl}_2 \cdot 4\text{H}_2\text{O}$, 1 mg EDTA disodium magnesium, $0.39 \text{ mg Na}_2\text{MoO}_4 \cdot 2\text{H}_2\text{O}$, $0.079 \text{ mg CuSO}_4 \cdot 5\text{H}_2\text{O}$, $0.22 \text{ mg ZnSO}_4 \cdot 7\text{H}_2\text{O}$, $0.05 \text{ mg Co(NO}_3)_2 \cdot 6\text{H}_2\text{O}$ per L of solution). The freshwater green microalgae *Scenedesmus obliquus* ATCC ® 11477TM was used as the test microorganism. Growth media amended with 10, 20, 40, 60 and 80% (v/v) of sample were tested with addition of a positive control (C+) medium and microalgae. The samples were incubated at 25°C in a growth chamber, under continuous shaking at 120 rpm using a 14:10 hours light: dark photoperiod and $5000 \text{ lux/ } 68 \mu\text{mol photons of}$

light intensity. A 5% carbon dioxide atmosphere was also provided during the lighting period. The duration of the test was 4 days. The pH of the samples was adjusted to 7.0 ± 0.1 prior to the test assessment. Fluorescence at 685 nm on a microplate reader (Biotek®, Citation 3) was measured as a surrogate for the estimation of the biomass at day 0, 1, 2, 3 and 4. Tests were executed per quadruplicates. Biomass results are expressed as a mean of cell density (cells/mL) \pm SD.

3. Results and discussion

3.1. Oxidation of synthetic NTO wastewater

The removal of synthetic NTO (NTO (sy)) by the UV/H₂O₂ technique was tested first. A solution of 250 mg L⁻¹ (1.92 mmol L⁻¹) of NTO in DI water was treated with 800 mg L⁻¹ (23 mmol L⁻¹) of H₂O₂ and UV light exposure for 10 hours; two control tests were also performed on the same solution in order to assess the effect of UV or H₂O₂ alone on the removal of NTO. Complete decomposition of NTO was achieved within 3 hours of reaction when the solutions were treated with the combination of UV/H₂O₂, while solutions treated separately by UV or H₂O₂ alone exhibited 7% and <1% reduction of the initial NTO, respectively (Fig. 2).

The solution pH was constant throughout treatment in the solutions treated with UV or H₂O₂ only, while it slightly increased to 3.4 ± 0.1 in the solution treated with UV/H₂O₂ (Fig.S5). Mass spectra obtained from samples collected after 4 hours of treatment confirmed the complete degradation of NTO by UV/H₂O₂ (Fig. S6); in fact, the spectrum showed no peak at m/z 129 for [NTO-H]⁻ but a significant peak at m/z 62, which is associated with nitrate (NO₃⁻) ion.

The total organic carbon (TOC) decreased following the same profile as the calculated NTO-[C], hence all organic carbon was converted to inorganic carbon (CO₂), and any carbon-containing intermediate was rapidly oxidized (Fig. 3a). The formation of CO₂ was confirmed through GC-MS analysis performed on gaseous samples collected from the headspace of the gas-

tight reactor where the NTO(sy) solution was treated ($800 \text{ mg L}^{-1} \text{ H}_2\text{O}_2$; UV light exposure 10 hours). The gaseous samples were collected at the beginning ($t=0$) (Fig. 4a) and after 3 hours of treatment (Fig. 4b), when NTO had been degraded by at least 99%. The other gaseous species detected in the system were oxygen (O_2) and nitrogen (N_2) gas (Fig. 4), which however did not show a significant relative increment compared to the results obtained from the blank system (Fig. S7).

The most abundant nitrogen by-products detected in the UV/ H_2O_2 treated NTO(sy) solution were nitrate (NO_3^-) and ammonium ions (NH_4^+) (Fig. 3b); nitrate concentrations increased as NTO was depleted in the test solution. Ammonium ion formation was observed after an initial delay and steadily increased as the NTO reached values below the detection limit ($<0.1 \text{ mg L}^{-1}$). Nitrite (NO_2^-) concentrations were constantly below the detection limit ($<0.05 \text{ mg L}^{-1}$), indicating rapid oxidation of this anion to nitrate. Nitrate and ammonium ions were also the main nitrogen by-products obtained from the photo-degradation of NTO in the presence of TiO_2 [26]. The nitrate formed during the reaction was attributed to the direct oxidation of nitrite from NTO denitration, while the ammonium ions were generated from the subsequent scission of the NTO ring, which is consistent with the delayed increase of ammonium ion concentrations found in the system [26, 27, 28].

The measured total nitrogen concentrations (TN) were constant over the entire treatment time, thus the formation of gaseous nitrogen (N_2) was negligible, as also confirmed by GC-MS analysis. The trend of the calculated nitrogen balance (TN-Calc) obtained by addition of all nitrogen species namely nitrate, nitrite, ammonium and NTO concentrations followed the trend of TN concentrations (Fig. 3b), which suggests that formation of other nitrogen-containing by-products is not significant.

3.2. NTO wastewater oxidation: Selection of reaction pH

The UV/H₂O₂ oxidation of the synthetic NTO performed satisfactorily, as the treatment effectively destroyed and mineralized the target compound. However, the dark color and turbidity of the industrial NTO wastewater (NTO(w)) may affect the UV irradiation [29], which is essential for the excitation of H₂O₂ and the generation of hydroxyl radicals (\cdot OH) acting as the primary oxidation agent for the target contaminant (NTO). Since pH is directly related to color and turbidity, acidification of the NTO wastewater was selected as a strategy to remove their interference on UV irradiation. Thus, an experimental study was conducted for selecting the appropriate pH level for the UV/H₂O₂ oxidation of NTO(w). The pH of the wastewater was adjusted to different values (2.3, 3.5, 4.0, 6.0, 8.0 \pm 0.1) by addition of sulfuric acid (H₂SO₄, 96% assay). Sulfuric acid was selected among others as it requires the least amount for pH adjustment compared to hydrochloric acid (HCl) and nitric acid (HNO₃). The UV/H₂O₂ oxidation of the raw NTO wastewater at unadjusted pH (12 \pm 0.1) was also investigated.

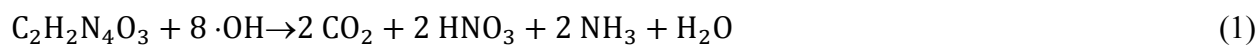
As the pH was adjusted from 12 to values as low as 2.3 \pm 0.1, the color of the wastewater changed from orange/red to light yellow (Fig. S8). Since NTO is an ionizable compound (pK_a 3.67 [9]), this behavior could be attributed to a pH induced speciation change. FTIR measurements of the NTO wastewater in the pH range 3.0-12 showed that the characteristic spectrum of NTO undergoes significant changes with increasing pH (Fig. S7). More explicitly, the peaks related to the amino (-NH, \sim 3500-3200 cm⁻¹) and carbonyl groups (-CO, \sim 1650 cm⁻¹) show a significant loss in intensity, attributed to ionization of the groups, that become positively charged with increasing pH. The ionization of the amino groups can cause changes in the color of the wastewater, as also observed for phenazines (C₁₂H₈N₂) and phenazinium derivatives [30]. In

particular, each step in the color change (brown to yellow) was associated with the number of amino groups available on the ring and their subsequent ionization.

After pH adjustment and addition of H_2O_2 , the wastewater was exposed to the UV light for 24 hours (Fig. 5). The initial H_2O_2 concentration used for the pH study tests was 3200 mg L^{-1} (95 mmol L^{-1}) and was based on practical guidelines reported in the literature [29, 31]. Accordingly, the amount of H_2O_2 to be used for treatment should be at least twice the concentration of the organic carbon to be oxidized which for NTO(w) is about 1600 mg L^{-1} (133 mmol L^{-1}).

The results obtained from the tests performed on the wastewater at different pH showed minimal to no removal of NTO within the established reaction time of 24 hours (Fig. 5). The highest percentage removal achieved was 23% for initial $\text{pH} = 2.3 \pm 0.1$, which can be correlated with the increased solution transparency at more acidic pH values (yellow color, Fig. S8), thus improving the UV light irradiation.

The low NTO conversion efficiency (23%) at the low pH (2.3 ± 0.1) was attributed either to a low oxidizing agent concentration ($\cdot\text{OH}$) due to a sub-stoichiometric dose of H_2O_2 or to a low conversion efficiency of the latter to $\cdot\text{OH}$ because of scavenging reactions. To test this hypothesis the amount of hydroxyl radicals required for the complete degradation of NTO in the wastewater was calculated through the stoichiometry of the theoretical UV/ H_2O_2 oxidation reaction of NTO assuming complete conversion of the contaminant to water, inorganic carbon and salts [32] and no scavenging reactions. Based to the results obtained from treatment of the synthetic NTO solution, nitrate, ammonium ions and carbon dioxide were the main products from the degradation of NTO; thus, the theoretical oxidation reaction of NTO by UV/ H_2O_2 , may be written as:





From the above equations, the theoretical stoichiometric requirement for the complete mineralization of NTO assuming no hydroxyl scavenging reactions is 8.0 mmol of $\cdot\text{OH}$ or 4.0 mmol H_2O_2 per mmol of NTO destructed. Hence the theoretical stoichiometric amount of $\cdot\text{OH}$ and H_2O_2 required to oxidize 64.6 mmol L^{-1} (8.4 g L^{-1}) of NTO, are 516.8 and $258.8 \text{ mmol L}^{-1}$ (8.8 g L^{-1}), respectively. The calculated H_2O_2 concentration was then applied to treat the NTO wastewater at $\text{pH } 3.0 \pm 0.1$ and 12.0 ± 0.1 (original pH), respectively. After 5.0 days and 12 hours of treatment, the NTO was removed by up to 97% of the initial concentration in the wastewater at $\text{pH}=3.0 \pm 0.1$, while only 8% of the initial concentration was removed at $\text{pH } 12.0 \pm 0.1$ (Fig. 6). The residual H_2O_2 concentration in the treated NTO wastewater at $\text{pH } 3.0 \pm 0.1$ was $455 \sim 500 \text{ mg L}^{-1}$ (13.4 mmol L^{-1}). Considering the conversion efficiency of NTO (97%), the calculated requirements of $\cdot\text{OH}$ and H_2O_2 are 501.3 and $251.0 \text{ mmol L}^{-1}$, respectively. The experimentally determined amount of H_2O_2 used (applied minus residual) is $245.4 \text{ mmol L}^{-1}$ and can deliver $490.8 \text{ mmol L}^{-1}$ of $\cdot\text{OH}$. Thus, the difference between the calculated and experimental quantities of $\cdot\text{OH}$ is 10.5 mmol L^{-1} corresponding to an error of less than 2.1% attributable to experimental and round off sources. Therefore, the hydroxyl radical generation efficiency of peroxide is very close to 100% and signifies the absence of hydroxyl radical scavenging reactions.

The attempted treatment of NTO wastewater by UV/ H_2O_2 under low pH compares favorably to similar treatment methods in the literature. Le Campion et al. [26] obtained degradation of 5 g L^{-1} of NTO in the presence of 0.4 g L^{-1} of TiO_2 after 8 days of continuous UV exposure (125 W). The results obtained from these tests, as illustrated in Fig. 6, confirmed that low pH (3.0 ± 0.1) represents a favorable condition for the treatment of NTO wastewater, as it significantly improved the efficiency of the UV irradiation and therefore the direct photolysis of

H₂O₂. In fact, when the pH of the wastewater was adjusted to 3.0 ± 0.1 , the initial irradiance of the UV light source was $0.9 \pm 0.01 \text{ mW cm}^{-2}$, while at the original pH, it was about $0.2 \pm 0.01 \text{ mW cm}^{-2}$. Moreover, as the treatment proceeded, and the color of the wastewater disappeared, the UV light irradiance in the wastewater at pH 3.0 ± 0.1 increased from $0.9 \pm 0.01 \text{ mW cm}^{-2}$ to about $8.0 \pm 0.5 \text{ mW cm}^{-2}$, which represents an increment of $\sim 90\%$ (Fig. 6). The increase of the UV irradiance in the wastewater at pH=12 was only $\sim 10\%$, with a final irradiance equal to $0.3 \pm 0.01 \text{ mW cm}^{-2}$.

Alkalinity is a parameter, closely associated to pH that must be considered in the application of UV/H₂O₂ oxidation [29]. The carbonic species responsible for carbonate (CO_3^{2-}) and bicarbonate (HCO_3^-) alkalinity may introduce alternative pathways for the degradation of the target organic contaminant, as these ions can consume hydroxyl radicals to generate fast reactive carbonate radicals [33]. The carbonate radicals are known to exert a significant inhibition for the UV/H₂O₂ process, especially in pH range 8.0-9.0 [34]. However, although the total alkalinity of the NTO wastewater was high (22 g L^{-1} as CaCO_3), the measured inorganic carbon (IC) content was quite low ($8 \pm 0.5 \text{ mg-C L}^{-1}$). At the pH of the raw NTO wastewater (12 ± 0.1), this amount of IC can contribute up to 70.8 mg/l as CaCO_3 of carbonate alkalinity, suggesting that the primary source of alkalinity originates from hydroxides. Upon acidification of the wastewater to the reaction pH (3.0 ± 0.1) which is well below the second equivalence point of the carbonate equilibria (pH ~ 4.5) even this small amount of carbonic species is expected to convert to CO_2 escaping the aqueous solution. Thus, under the experimental conditions, the effect of the carbonic species on the removal of NTO by UV/H₂O₂ oxidation is negligible.

Similar to the synthetic NTO solution, the degradation of NTO in the actual wastewater followed the proposed theoretical chemical reactions [Eqs. (1), (2)]; the NTO-[C] was converted to inorganic carbon (CO_2) (Fig. 7a), while the NTO-[N] was mostly converted to ammonium and

nitrate ions (Fig. 7b). The measured nitrite concentrations were $\leq 0.5 \text{ mg L}^{-1}$ due to its rapid oxidation to nitrate.

The successful mineralization of the original NTO was assessed through toxicological tests performed on the water post-treatment with *S.Obliquus* (Fig. S10a); the outcome of the tests showed decreased toxicity compared to the untreated wastewater, as the growth of the microalgae showed no inhibition up to 20% of the original sample. Upon neutralization, this dilution level can serve as the basis for selecting the appropriate ammonia and nitrate loadings that can be fed to algal bioreactors without any adverse toxicity effects. The inhibition exhibited for higher percentages may be attributed to the residual ammonia and nitrate in the water post-treatment [35].

3.3. NTO wastewater oxidation: NTO concentration effects

In the second part of this study, the effect of the initial NTO concentration on UV/H₂O₂ oxidation was also investigated. For this purpose, several tests were performed at different dilution ratios (60, 16, 6.0, 4.5 and 4.0) to the industrial wastewater; the initial NTO concentrations obtained were 270, 500, 1300, 1700 and 1900 mg L⁻¹ (2.07, 3.84, 10.0, 13.0 and 14.6 mmol L⁻¹) with initial pH of 10.0, 10.9, 11.3, 11.5, and 11.7±0.1, respectively. The pH of the diluted wastewater was adjusted to 3.0±0.1 and the H₂O₂ concentration was fixed at 1500 mg L⁻¹ (44 mmol L⁻¹), which represents the average concentration obtained through calculation of the stoichiometric H₂O₂ concentrations according to Eq.(1), (2). In addition, two control tests were also performed in order to assess NTO removal in the wastewater by H₂O₂ or UV alone (NTO(i)= 1900 mg L⁻¹;14.6 mmol L⁻¹).

According to the results obtained (Fig. 8), when the initial NTO(w) concentration was between 200-500 mg L⁻¹, complete NTO removal was achieved within 10 hours treatment, while for concentrations higher than 1300 mg L⁻¹, 24 to 48 hours of treatment were required in order to

achieve 99% removal. The NTO removal percentages obtained for the application of UV or H₂O₂ only were less than 10% (Fig. 8), which highlight the essential role of peroxide in generating the hydroxyl radicals ($\cdot\text{OH}$) acting as the oxidizing agent responsible for the degradation of NTO, as was also observed for the synthetic NTO solution (Fig.2).

After an initial drop, the pH was overall constant during the reaction time (Fig. S11) in all tests; the initial decrease of the pH can be attributed to the rapid oxidation of residual nitrite in solution to nitrate and subsequent formation of nitric acid. The H₂O₂ concentrations (Fig. S12) decreased following the same trend of the NTO concentrations (Fig. 8) which indicates that the $\cdot\text{OH}$ from dissociation of H₂O₂ are immediately depleted for oxidation of the target compound. The residual peroxide concentrations detected in the water post-treatment were 80, 62, 10, 3 and 1 mg L⁻¹ for initial NTO(w) concentrations of 270, 500, 1300, 1700 and 1900 mg L⁻¹, respectively.

Since H₂SO₄ was used for pH adjustment in all tests performed, it is necessary to take into account the possible contribution of sulfate radicals (SO₄ \cdot^-) in the oxidation of NTO. In fact, it is known that in presence of H₂SO₄, $\cdot\text{OH}$ can react with hydrogen sulfate ions (HSO₄ $^-$) to generate SO₄ \cdot^- , which are capable of reacting with organic compounds. For this reason, control experiments in presence of other acids (HCl, HNO₃) were performed using the same conditions applied to the kinetic tests in Fig. 8. The degradation kinetics of NTO in presence of H₂SO₄ did not show significant differences compared to other acids (HCl, HNO₃) (Fig. S13). This could be attributed to the low reactivity of HO \cdot toward HSO₄ $^-$ ($k=3.5 \times 10^5 \text{ M}^{-1} \text{ s}^{-1}$) [36] as well as low reactivity of SO₄ \cdot^- towards the neutral form of ionizable compounds [37, 38]. Thus, the effect of the SO₄ \cdot^- on the degradation of NTO by UV/H₂O₂ for the conditions tested can be neglected.

The NTO-[C] was completely mineralized to inorganic carbon, as indicated by the measured TOC concentrations (Fig. 9). The calculated carbon concentration from the NTO

followed the same trend as the analyzed TOC, which indicated that any intermediate organic carbon by-products were not stable enough to survive the oxidation. MS spectra obtained for several samples collected at the end of each treatment time (Fig. S14) also confirmed the complete degradation of NTO; the most significant peaks identified at m/z 62 and m/z 97 were associated with nitrate and sulfuric acid, respectively.

As previously observed, the main nitrogen by-products were nitrate and ammonium ions, which increased with the initial NTO concentration (Fig. 10a, b). The ammonium ions represented a significant residual from the degradation of NTO as showed through tests performed for both wastewater (Fig 7b; Fig. 10a) and synthetic solution (Fig. 3b). It is known that ammonium could undergo direct oxidation under UV irradiation or reaction with $\cdot\text{OH}$ [39] leading to increase in nitrite and nitrate concentrations. However, in our study, the ammonium concentrations increased with a stable trend as the NTO concentrations decreased; this outcome can be most likely attributed to the initial low pH (3.0 ± 0.1) and the persistent acidic conditions during the treatment ($\text{pH} = 3.0$ - 2.0) (Fig.S11). In fact, the removal of ammonia by UV/ H_2O_2 was found to be strictly favored at alkaline conditions ($\text{pH} \geq 7.0$), whereas only a small fraction ($< 2 \text{ mg-N L}^{-1}$) was oxidized at $\text{pH} \leq 7.0$ [40]. This result was also confirmed through control tests (Fig.S15) performed on a solution of pure ammonia (100 mg-N L^{-1} as $\text{NH}_4\text{-[N]}$) using the same conditions applied for the treatment of NTO ($\text{pH} = 3.0 \pm 0.1$; $\text{H}_2\text{O}_2 = 1500 \text{ mg L}^{-1}$). The outcome of the tests showed that the ammonia was stable over 24 hours of continuous UV irradiation, both in presence and absence of H_2O_2 with less than 1% of ammonia oxidized to nitrite and nitrate.

The nitrite concentrations instead decreased to values below 1 mg L^{-1} within the first 5 hours of treatment (Fig. 11); in fact, the addition of H_2O_2 to the system also contributed to the oxidation of the nitrite ions to nitrate, also shown by results confirmed from the control tests. It is

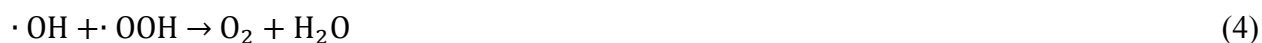
known that H_2O_2 is a powerful oxidizer in an acidic solution, and it has been proved that at pH as low as 4.0-3.0, it can significantly increase the oxidation rate of nitrite to nitrate [41].

The nitrogen mass balance was obtained by addition of nitrogen from nitrite, nitrate, ammonium and NTO over the entire treatment time. The close agreement between the calculated and measured total nitrogen (TN) concentrations indicates that the formation of gaseous nitrogen was insignificant (Fig. 12).

3.4. NTO wastewater oxidation: H_2O_2 concentration effect

The effect of the initial H_2O_2 concentration on NTO removal in the wastewater was assessed by performing additional experiments on diluted wastewater with an initial NTO concentration of 1900 mg L^{-1} (14.6 mmol L^{-1}) and pH adjusted according to the conditions applied in former tests ($\text{pH(i)} = 3.0 \pm 0.1$). The H_2O_2 concentrations tested were 800, 1500, 3200, 4500 and 6000 mg L^{-1} (23.5, 44.1, 94.1, 132 and 176 mmol L^{-1}) with reaction time fixed at 48 hours.

As the initial H_2O_2 concentration increased from 1500 mg L^{-1} to 6000 mg L^{-1} , the reaction time in order to achieve 99% removal of NTO decreased from 48 hours to about 12 hours, while only 40% of the initial NTO was removed with 800 mg L^{-1} of H_2O_2 after 36 hours of treatment (Fig.13). In general, the removal efficiency of organic compounds with UV/ H_2O_2 oxidation increases with the initial H_2O_2 as more $\cdot\text{OH}$ radicals are generated [25, 32, 33, 42]. However, excess of H_2O_2 can cause significant scavenger effect on the highly reactive free radicals through competitive reactions (Eq (3) - (5) [46-46]):



From the results in Fig. 13, it is clear that the degradation rate of NTO did not show significant improvement for H_2O_2 concentrations $\geq 3200 \text{ mg L}^{-1}$, in fact the time to oxidize 99% of the NTO did not change despite the initial H_2O_2 concentration applied (Fig. 14). Such outcome suggests that 3200 mg L^{-1} represents the threshold value for the achievement of the maximum efficiency by the mineralization process and therefore the optimal concentration for the removal of 1900 mg L^{-1} of NTO. The resulting optimal NTO/ H_2O_2 molar ratio for treatment of the wastewater is about 0.2, which is less than the stoichiometric ratio of 0.25 suggested by Eqs. (1)-(2). Thus, scavenger effects due to excess of H_2O_2 should not be significant for ratios below this value.

Although H_2O_2 concentrations $\geq 3200 \text{ mg L}^{-1}$ resulted in residual H_2O_2 in the water post-treatment from about 100 to over 1000 mg L^{-1} , the scavenger effects induced by the excess of peroxide did not show a significant decline in the degradation rate of NTO (Fig. 14). In fact, scavenging of the free radicals in UV/ H_2O_2 systems is usually predominant when the time required degrading the target organics becomes longer with the increase of H_2O_2 concentration [42, 43].

4. Conclusions

The results obtained from the present work indicate that UV/ H_2O_2 oxidation is a promising technique for treatment of NTO wastewater streams at high concentration; the efficiency of the treatment was mainly dependent on the initial pH of the wastewater as well as the applied hydrogen peroxide concentration. The pH had a major influence on the color of the wastewater, which directly affects the extent of the UV irradiation and therefore the photolysis of H_2O_2 . In particular, low pH of 3.0 ± 0.1 was proved to be favorable for the complete mineralization of NTO in the wastewater (8.4 g L^{-1}), at the stoichiometric hydrogen peroxide concentration of 8.8 g L^{-1} .

Moreover, UV and a hydrogen peroxide concentration of 1500 mg L^{-1} in combination with a low $\text{pH} = 3.0 \pm 0.1$ achieved a total removal of NTO in the range of $250\text{-}1900 \text{ mg L}^{-1}$.

The total organic carbon analysis together with the characterization of the gaseous by-products showed that all the carbon from NTO was converted to inorganic carbon (CO_2). The same result was also confirmed though MS analysis obtained from samples post-treatment. On the other hand, analysis of the nitrogen by-products revealed that the organic nitrogen from NTO was mainly involved in the formation of nitrate and ammonium ions. Therefore, the UV/ H_2O_2 oxidation was shown to be a suitable treatment to achieve complete mineralization of contaminated NTO wastewater and recovery of valuable nutrients that can be used for supporting algal biomass growth for biofuel/biogas generation.

References

- [1] S. DeFisher, D. Pfau, C. Dyka, Insensitive Munitions Modeling Improvement Efforts, Army Armament Research Development and Engineering Center (2010) Picatinny Arsenal, NJ
- [2] J.P. Agrawal, Some new high energetic materials and their formulations for specialized applications, *Propellants Explos. Pyrotech.* 30 (2005) 316-328
- [3] A.K. Sikder, N. Sikder, A review of advanced high performance, insensitive and thermally stable energetic materials emerging for military and space applications, *J. Hazard. Mater.* 112 (2004) 1-15
- [4] D.L. Kaplan, A.M. Kaplan, Mutagenicity of 2, 4, 6-trinitrotoluene-surfactant complexes. *Bull. Environ. Contam. Toxicol.* 28 (1982), 33-38
- [5] T. Maeda, R. Nakamura, K. Kadokami, H.I. Ogawa, Relationship between mutagenicity and reactivity or biodegradability for nitroaromatic compounds, *Environ. Toxicol. Chem.* 26 (2007) 237-241.
- [6] P. A. Picatinny, Army approves safer explosive to replace TNT, *Federal Information & News Dispatch, Inc, Lanham* (2010)
- [7] A. Becuwe and A. Delclos, Low-sensitivity explosive compounds for low vulnerability warheads, *Propellants Explos. Pyrotech.* 18 (1993) 1-10
- [8] M.V. Haley, R.G. Kuperman, R.T. Checkai, Aquatic Toxicity of 3-Nitro-1, 2,4-Triazol-5-One, Edgewood Chemical Biological Center Aberdeen Proving Ground MD Research and Technology (2009)
- [9] K. Dontsova, M. Brusseau, J. Arthur, N. Mark, S. Taylor, J. Lever, M. Walsh, R. Pesce-Rodriguez, J. Simunek, Dissolution of NTO, DNAN and Insensitive Munitions Formulation and their fates in soils. US Army Corps of Engineers, Final Report ERDC/CRREL TR-14-23, (2014)
- [10] M.V. Haley, R.G. Kuperman, R.T. Checkai, Aquatic Toxicity of 3-Nitro-1,2,4-triazol-5-one Edgewood Chemical Biological Center, U.S. Army Research, Development and Engineering Command, Aberdeen Proving Ground, MD (2009) 21010-25424
- [11] J.K. Stanley, G.R. Lotufo, J.M. Biedenbach, P. Chappell, K.A. Gust, Toxicity of the conventional energetics TNT and RDX relative to new insensitive munitions constituents DNAN and NTO in *Rana pipiens* tadpoles, *Environ. Toxicol. Chem.* 34 (2015) 873-879
- [12] S. Wallace, The Subchronic Oral Toxicity of 3-Nitro-1,2,4-triazol-5-one (NTO) in Rats (*Rattus norvegicus*) U.S. Army Center for Health Promotion and Preventive Medicine (2011)

- [13] L. Le Campion, C. Giannotti, J. Ouazzani, Microbial remediation of NTO in aqueous industrial wastes, *FEMS Microbiol. Lett.* 176 (1999a) 197–203
- [14] M. Krzmarzick, R. Khatiwada, C.I. Olivares, L. Abrell, R. Sierra-Alvarez, J. Chorover, A. Field, Biotransformation and degradation of the Insensitive Munitions Compound, 3-Nitro-1,2,4-triazol-5-one, by Soil Bacterial Communities, *Env. Sci. Technol.* 49 (2015) 5681-5688
- [15] T. Richard, J. Weidhaas, Degradation, sorption and phytoremediation of IMX-101 explosive formulation constituents: 2, 4-dinitroanisoie (DNAN), 3-nitro-1, 2, 4-triazol-5-one (NTO), and nitroguanidine, *J. Hazard. Mater.* 280 (2014), 561-9
- [16] E.S. Salama, M.B. Kurade, R.A. Abou-Shanab, M.M. El-Dalatony, I.S. Yang, B. Min, B.H. Jeon, B. H., Recent progress in microalgal biomass production coupled with wastewater treatment for biofuel generation, *Renew. Sust. Energ. Rev.*, 79(2017), 1189-1211
- [17] P. Bose, W.H. Glaze, S.D. Maddox, Degradation of RDX by various advanced oxidation processes: I. Reaction rates, *Water Res.* 32 (1998) 997-1004
- [18] K.D. Zoh, M.K. Stenstrom, Fenton Oxidation of hexahydro-1,3,5- trinitro-1,3,5-triazine (RDX) and octrahydro-1,3,5,7-tetranitro-1,3,5,7-tetrazocine, *Water Res.* 36 (2002) 1331-1341
- [19] K. Ayoub, E.D. Van Hullebush, M. Cassir, A. Bermond, Application of advanced oxidation processes for TNT removal, *J. Hazard. Mater.* 178 (2010) 10-28
- [20] G.V Buxton, C.L Greenstock, W.P Helman, A.B Ross, Critical review of rate constants for reactions of hydrated electrons, hydrogen atoms and hydroxyl radicals in aqueous solution, *J. Phys. Chem. Ref. Data*, 17 (1988), 513-886
- [21] J. R. Bolton, S. R. Cater, Homogeneous photodegradation of pollutants in contaminated waters. In *Aquatic and Surface Photochemistry*; G.R. Helz, R. G. Zepp, D. G. Crosby, Eds.; Lewis Publishers: Boca Raton, FL, (1994) 67-490
- [22] I. Nicole, J. De Laat, M. Dore, Evaluation of reaction rate constants of OH radicals with organic compounds in diluted aqueous solutions using H₂O₂/UV process. In *Proc. 10th Ozone World Congr.* 1 (1991) 279–290
- [23] A. Hirvonen, T. Tuhkanen, P. Kalliokoski, Treatment of TCE- and TeCE-contaminated groundwater using UV/H₂O₂ and O₃/H₂O₂ oxidation processes. *Water Sci. Technol.* 33 (1996) 67–73
- [24] H. Bischof, C. Höfl, C. Schönweitz, G. Sigl., B. Wimmer, D. Wabner, UV-activated hydrogen peroxide for ground and drinking water treatment – development of technical process. In *Proc.*

Reg. Conf. Ozone, UV-light, AOPs Water Treatm., Amsterdam, Netherlands, 24–26 (1996) 117–131

[25] F.S Garcia Einschlag, J. Lopez, L. Carlos, A.L. Capparelli, Evaluation of the efficiency of photodegradation of nitroaromatics applying the UV/H₂O₂ technique, *Environ. Sci. Technol.* 36 (2002) 3936–3944

[26] L. Le Campion, C. Giannotti, J. Ouazzani, Photocatalytic degradation of nitro-1,2,4-triazol-3-one (NTO) in aqueous suspension of TiO₂, comparison with fenton oxidation, *Chemosphere*, 38 (1999b) 1561-1570

[27] D.C. Schmelling, K.A. Gray, Photocatalytic transformation and mineralization of 2, 4, 6-trinitrotoluene (TNT) in TiO₂ slurries, *Water Res.* 29 (1995) 2651-2662

[28] G. Singh, I. P. Singh Kapoor, S. K. Tiwari, P. S. Felix, Studies on energetic compounds Part 16. Chemistry and decomposition mechanisms of 5-nitro-2, 4-dihydro-3H-1, 2, 4-triazole-3-one (NTO), *J. Hazard. Mater.* B81 (2001) 67-82

[29] S. Kommineni, J. Zoeckler, A. Stocking, P.S. Liang, A. Flores, R. Rodriguez, T. Browne, P.R. Roberts, A. Brown, 3.0 Advanced Oxidation Processes, Treatment Technologies for Removal of Methyl Tertiary Butyl Ether (MTBE) from Drinking Water: Air Stripping, Advanced Oxidation Process, Granular Activated Carbon, Synthetic Resin Sorbents. Second ed., National Water Research Institute (2000) 109–208

[30] G.A. Swan, The chemistry of heterocyclic compounds, Phenazines, Intescience publishers Inc, NY, 1957

[31] R. Munter, Advanced oxidation processes—current status and prospects, *Proc. Estonian Acad. Sci. Chem* 50.2 (2001) 59-80

[32] N. López, S. Plaza, A. Afkhami, P. Marco, J. Giménez, S. Esplugas, Treatment of Diphenhydramine with different AOPs including photo-Fenton at circumneutral pH, *Chem. Eng. J.* 318 (2016), 112-120

[33] Y. Liu, X. He, X. Duan, Y. Fu, D.D. Dionysiou, Photochemical degradation of oxytetracycline: influence of pH and role of carbonate radical, *Chem. Eng. J.*, 276(2015), 113-121

[34] M. Muruganandham, R.P.S Suri, S. Jafari, M. Sillanpää, L. Gang-Juan, J.J. Wu, M. Swaminathan, Recent Developments in Homogeneous Advanced Oxidation Processes for Water and Wastewater Treatment, *Int. J. Photoenergy* (2014), 821674

[35] A. Konig, H. W. Pearson, Ammonia toxicity to algal growth in waste stabilization ponds. *Water Science and Technology*, 19(1987), 115-122

- [36] F. S. García Einschlag, J. Lopez, L. Carlos, A. L. Capparelli, A. M. Braun, E. Oliveros, Evaluation of the efficiency of photodegradation of nitroaromatics applying the UV/H₂O₂ technique. *Environ. Sci. Technol.*, 36(2002), 3936-3944
- [37] J. Criquet, N.K.V. Leitner, Degradation of acetic acid with sulfate radical generated by persulfate ions photolysis, *Chemosphere*, 77(2009), 194-200.
- [38] Y. Liu, X. He, Y. Fu, D.D. Dionysiou, Kinetics and mechanism investigation on the destruction of oxytetracycline by UV-254 nm activation of persulfate *J. Hazard. Mater.*, 305 (2016), 229-239.
- [39] A. Wang, J.G. Edwards, J.A Davies, Photo oxidation of aqueous ammonia with titania based heterogeneous catalysts, *Sol. Energy*, 52(1994), 459–466
- [40] L. Huang, L. Liang, D. Wenbo, L. Yan, H. Huiqi, Removal of Ammonia by OH Radical in Aqueous Phase, *Env. Sci. Technol*, 42 (2008), 8070-8075
- [41] D.J. Thomas, M. Vanderschuren, M. Barigand, Influence of acidity on the oxidation rate of nitrous acid by hydrogen peroxide, *J. Chem. Phys.* 95 (1998) 532-535
- [42] W. Zhang, X. Xiao, T. An, Z. Song, J. Fu, G. Sheng, M. Cui, Kinetics, degradation pathway and reaction mechanism of advanced oxidation of 4-nitrophenol in water by a UV/H₂O₂ process, *J. Chem. Technol. Biotechnol.*, 78(2003), 788-794
- [43] G.S. Wang, S.T. Hsieh, C.S. Hong, Destruction of humic acid in water by UV light—catalyzed oxidation with hydrogen peroxide. *Water Res.*, 34(2000), 3882-3887
- [44] A.K. De, B. Chaudhuri, S. Bhattacharjee, B.K. Dutta, Estimation of ·OH radical reaction rate constants for phenol and chlorinated phenols using UV/H₂O₂ photo-oxidation, *J. Hazard. Mater.* , 64(1999), 91-104
- [45] H. Shemer, K. G. Linden, Degradation and by-product formation of diazinon in water during UV and UV/H₂O₂ treatment, *J. Hazard. Mater.*, 136(2006), 553-559.
- [46] J.L. Wang., L.J. Xu, Advanced oxidation processes for wastewater treatment: formation of hydroxyl radical and application, *Crit. Rev. Env. Sci. Technol.* (2012), 42(3), 251-325.

Figure Captions

Fig. 1. Mass spectrum recorded from NTO wastewater under negative-ion-generating conditions.

Fig. 2. NTO concentrations for different treatment conditions vs time in NTO(sy); NTO (i)=250 mg L⁻¹, UV, H₂O₂=800 mg L⁻¹, pH (i) =3.0±0.1. Error bars represent standard deviation from two replicates.

Fig. 3. (A) TOC, NTO-[C] and (B) NTO-[N], NO₃-[N], NH₄-[N] and total nitrogen (measured and calculated) concentrations vs time in NTO(sy); NTO (i) =250 mg L⁻¹, H₂O₂=800 mg L⁻¹, pH (i) =3.0±0.1. Error bars represent standard deviation from two replicates.

Fig. 4. Mass spectrum of gaseous sample from oxidation of NTO(sy) at (A) 0 and (B) 3 hours of treatment; NTO (sy) =250 mg L⁻¹, H₂O₂=800 mg L⁻¹, pH (i) =3.0±0.1.

Fig. 5. NTO concentrations vs time for different initial pH (2.3, 3.5, 4.0, 6.0, 8.0, 12) in NTO(w); NTO(i) =8400 mg L⁻¹, UV, H₂O₂=3200 mg L⁻¹.

Fig. 6. NTO concentrations and UV irradiance vs time for different initial pH (3.0±0.1, 12±0.1) in NTO(w); NTO (i) =8400 mg L⁻¹, UV, H₂O₂=8800 mg L⁻¹. Error bars represent standard deviation from two replicates.

Fig. 7. (A) TOC, NTO-[C] and (B) NTO-[N], NO₃-[N], NH₄-[N] and total nitrogen (measured and calculated) concentrations vs time in NTO(w); NTO(i)=8400 mg L⁻¹, H₂O₂=8800 mg L⁻¹, pH(i) =3.0±0.1. Error bars represent standard deviation from two replicates.

Fig. 8. NTO(w) concentrations vs time for different NTO concentrations (270, 500, 1300, 1700, 1900 mg L⁻¹); UV, H₂O₂=1500 mg L⁻¹, pH (i) =3±0.1. Error bars represent standard deviation from three replicates.

Fig. 9. TOC concentrations vs time in NTO(w) for different NTO concentrations (270, 500, 1300, 1700, 1900 mg L⁻¹); UV, H₂O₂=1500 mg L⁻¹, pH (i) =3.0±0.1. Solid curves represent the calculated NTO-[C] concentrations. Error bars represent standard deviation from three replicates.

Fig. 10. (A) NH₄-[N] and (B) NO₃-[N] concentrations in NTO(w) vs time for different NTO concentrations (270, 500, 1300, 1700, 1900 mg L⁻¹); UV, H₂O₂=1500 mg L⁻¹, pH(i)=3.0±0.1. Error bars represent standard deviation from three replicates.

Fig. 11. NO₂-[N] concentrations in NTO(w) vs time for different NTO concentrations (270, 500, 1300, 1700, 1900 mg L⁻¹); (A) inset for NO₂-[N] concentrations between 0-1.2 mg L⁻¹ in the time window 0-30 hours; UV, H₂O₂=1500 mg L⁻¹, pH(i)=3.0±0.1. Error bars represent standard deviation from three replicates.

Fig. 12. Total N concentrations in NTO(w) vs time for different NTO concentrations (270, 500, 1300, 1700, 1900 mg L⁻¹); UV, H₂O₂=1500 mg L⁻¹, pH (i) =3.0±0.1. Dotted curves represent the calculated nitrogen balance. Error bars represent standard deviation from three replicates.

Fig. 13. NTO(w) concentrations vs time for different hydrogen peroxide concentrations (800, 1500, 3200, 4500, 6000 mg L⁻¹); UV, pH (i) = 3.0±0.1, NTO (w) = 1900 mg L⁻¹. Error bars represent standard deviation from three replicates.

Fig. 14. NTO removal efficiencies for different initial H₂O₂ concentrations at 12 hours reaction time; UV, pH (i) = 3.0±0.1, NTO(i) = 1900 mg L⁻¹. Error bars represent standard deviation from three replicates.

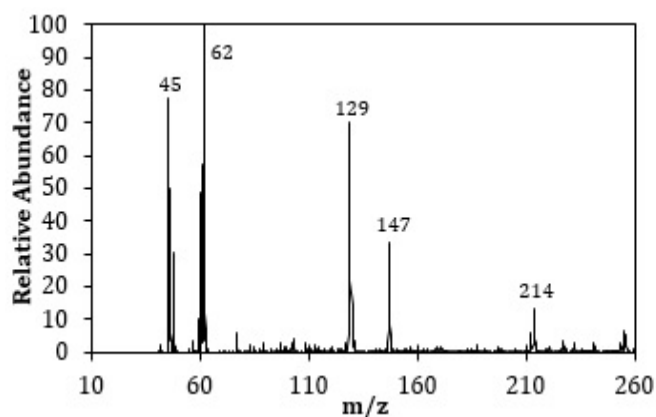


Fig. 1. Mass spectrum recorded from NTO wastewater under negative-ion-generating conditions.

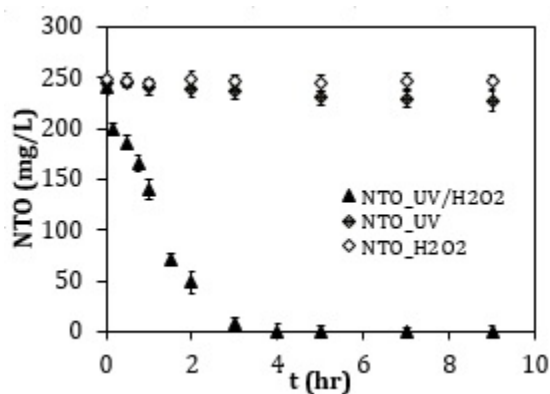


Fig. 2. NTO concentrations for different treatment conditions vs time in NTO(sy); NTO (i)=250 mg L⁻¹, UV, H₂O₂=800 mg L⁻¹, pH (i) =3.0±0.1. Error bars represent standard deviation from two replicates.

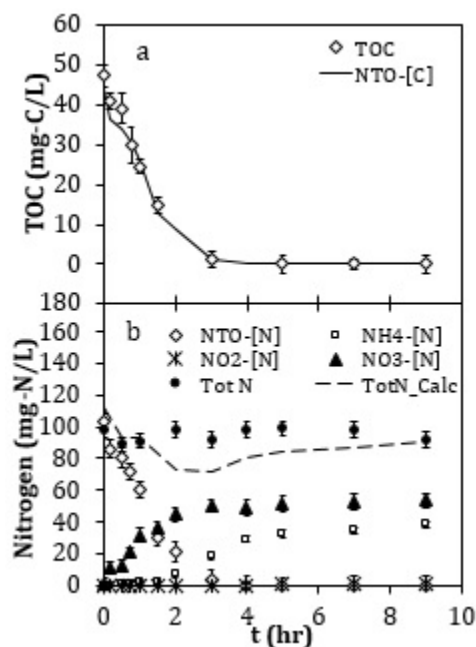


Fig. 3. (a) TOC, NTO-[C] and (b) NTO-[N], NO₃-[N], NH₄-[N] and total nitrogen (measured and calculated) concentrations vs time in NTO(sy); NTO (i) =250 mg L⁻¹, H₂O₂=800 mg L⁻¹, pH (i) =3.0±0.1. Error bars represent standard deviation from two replicates.

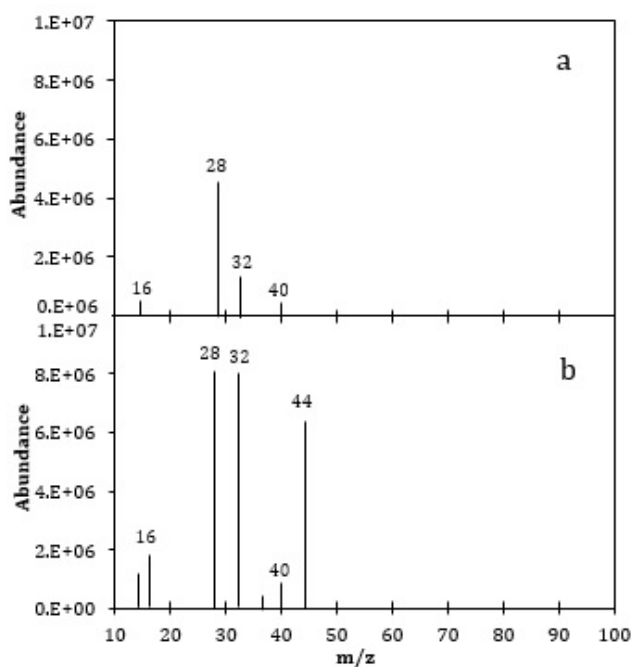


Fig. 4. Mass spectrum of gaseous sample from oxidation of NTO(sy) at (A) 0 and (B) 3 hours of treatment; NTO (i) =250 mg L⁻¹, H₂O₂=800 mg L⁻¹, pH (i) =3.0±0.1.

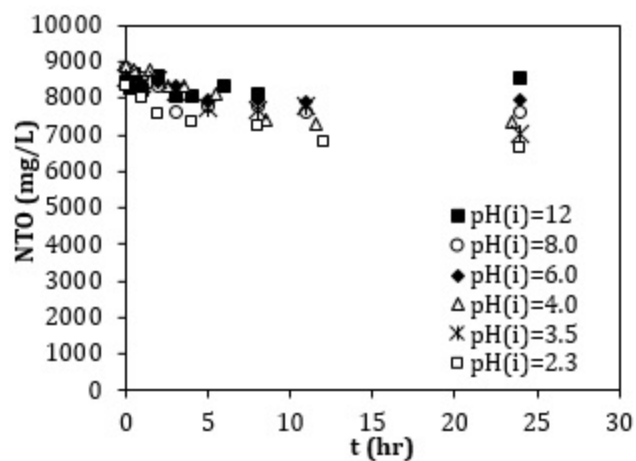


Fig. 5. NTO concentrations vs time for different initial pH (2.3, 3.5, 4.0, 6.0, 8.0, 12) in NTO(w); NTO(i) = 8400 mg L⁻¹, UV, H₂O₂ = 3200 mg L⁻¹.

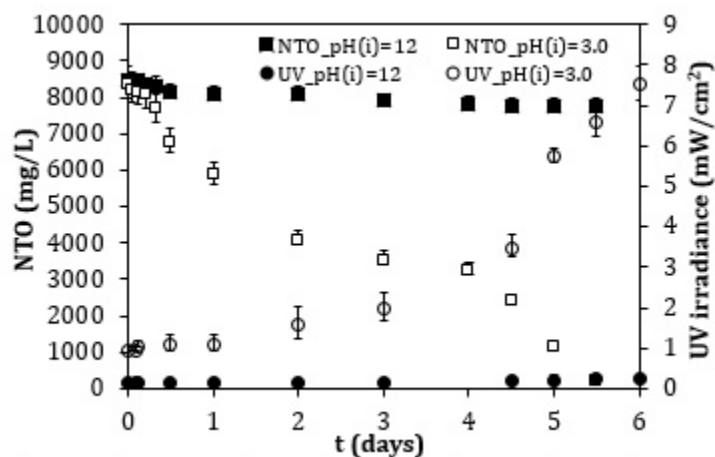


Fig. 6. NTO concentrations and UV irradiance vs time for different initial pH (3.0±0.1, 12±0.1) in NTO(w); NTO (i) = 8400 mg L⁻¹, UV, H₂O₂ = 8800 mg L⁻¹. Error bars represent standard deviation from two replicates.

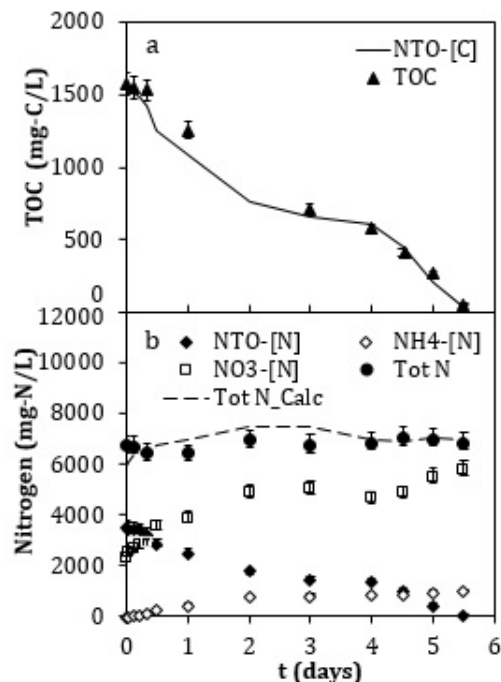


Fig. 7. (a) TOC, NTO-[C] and (b) NTO-[N], NO_3 -[N], NH_4 -[N] and total nitrogen (measured and calculated) concentrations vs time in NTO(w); NTO(i)=8400 mg L⁻¹, H_2O_2 =8800 mg L⁻¹, pH(i)=3.0±0.1. Error bars represent standard deviation from two replicates.

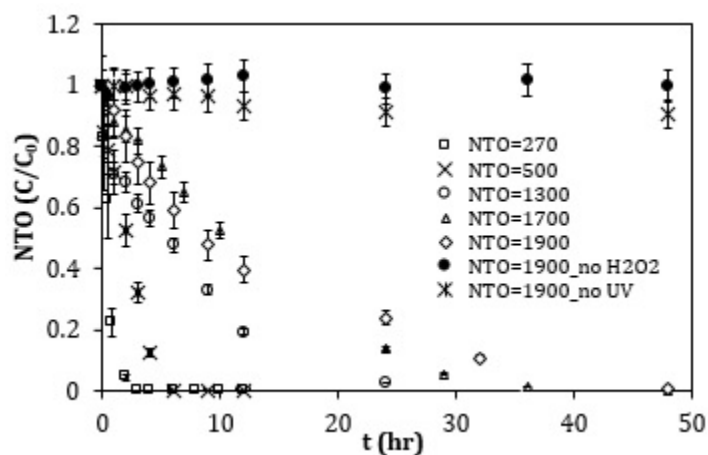


Fig. 8. NTO concentrations vs time in NTO(w) for different NTO concentrations (270, 500, 1300, 1700, 1900 mg L⁻¹); UV, H_2O_2 =1500 mg L⁻¹, pH (i) =3±0.1. Error bars represent standard deviation from three replicates.

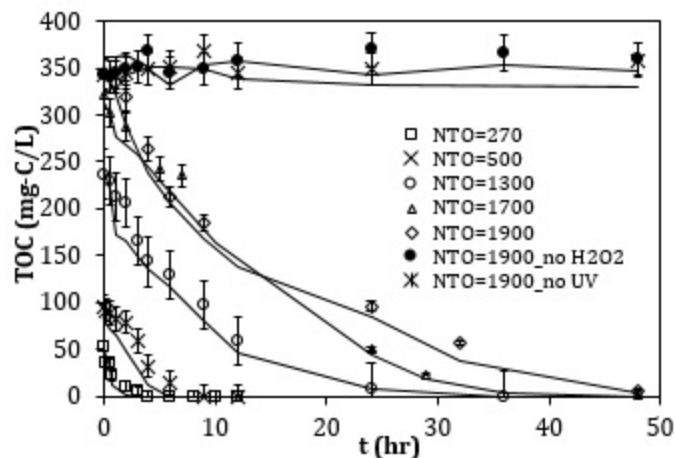


Fig. 9. TOC concentrations vs time in NTO(w) for different NTO concentrations (270, 500, 1300, 1700, 1900 mg L⁻¹); UV, H₂O₂=1500 mg L⁻¹, pH (i) =3.0±0.1. Solid curves represent the calculated NTO-[C] concentrations. Error bars represent standard deviation from three replicates.

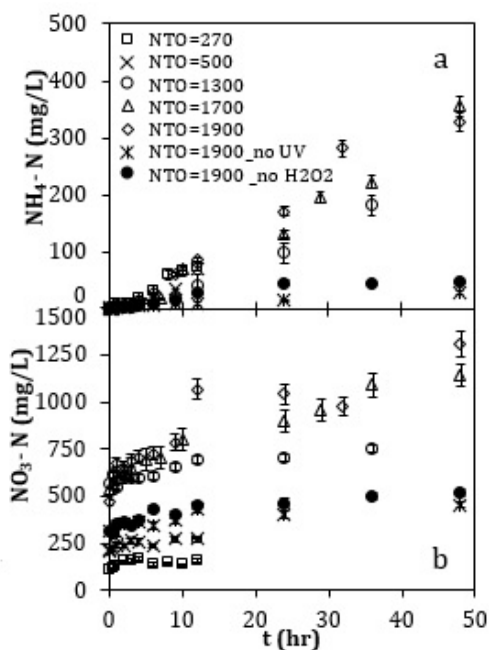


Fig. 10. (a) NH₄-[N] and (b) NO₃-[N] concentrations in NTO(w) vs time for different NTO concentrations (270, 500, 1300, 1700, 1900 mg L⁻¹); UV, H₂O₂=1500 mg L⁻¹, pH(i)=3.0±0.1. Error bars represent standard deviation from three replicates.

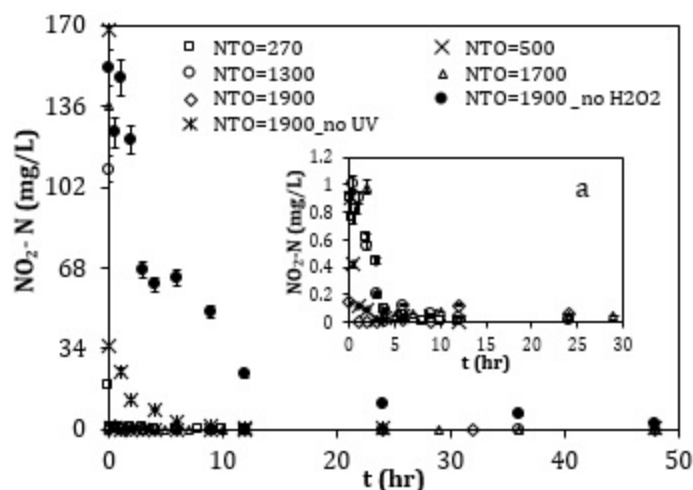


Fig. 11. $\text{NO}_2\text{-N}$ concentrations in NTO(w) vs time for different NTO concentrations (270, 500, 1300, 1700, 1900 mg L^{-1}); (a) inset for $\text{NO}_2\text{-N}$ concentrations between 0-1.2 mg L^{-1} in the time window 0-30 hours; UV, $\text{H}_2\text{O}_2=1500 \text{ mg L}^{-1}$, $\text{pH}(i)=3.0\pm0.1$. Error bars represent standard deviation from three replicates.

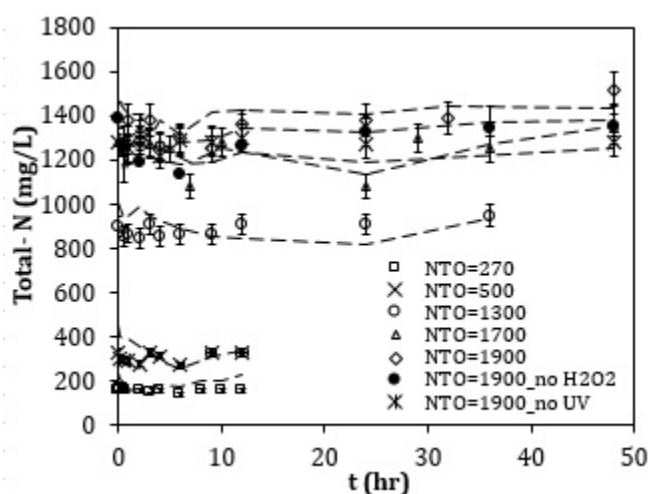


Fig. 12. Total N concentrations in NTO(w) vs time for different NTO concentrations (270, 500, 1300, 1700, 1900 mg L^{-1}); UV, $\text{H}_2\text{O}_2=1500 \text{ mg L}^{-1}$, $\text{pH}(i)=3.0\pm0.1$. Dotted curves represent the calculated nitrogen balance. Error bars represent standard deviation from three replicates.

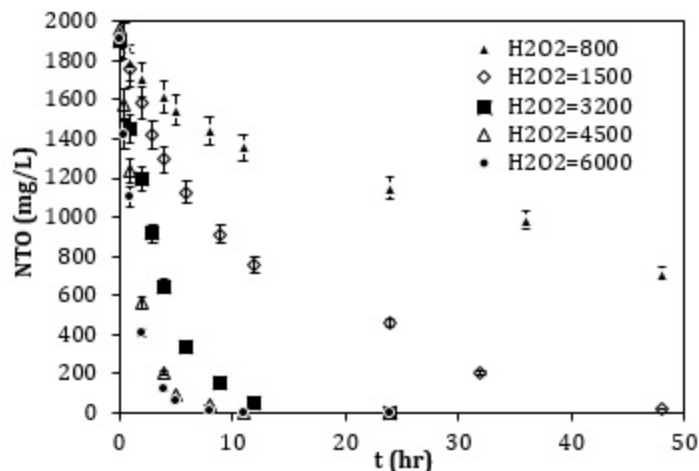


Fig. 13. NTO concentrations vs time in NTO(w) for different H_2O_2 concentrations (800, 1500, 3200, 4500, 6000 mg L^{-1}); UV, pH (i) = 3.0 ± 0.1 , $\text{NTO}(i) = 1900 \text{ mg L}^{-1}$. Error bars represent standard deviation from three replicates.

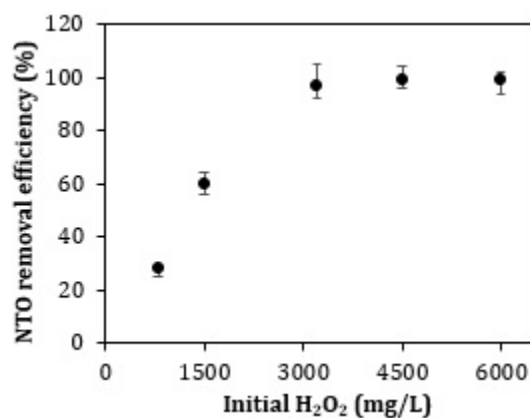


Fig. 14. NTO removal efficiencies for different initial H_2O_2 concentrations (800, 1500, 3200, 4500, 6000 mg L^{-1}) at 12 hours reaction time; UV, pH (i) = 3.0 ± 0.1 , $\text{NTO}(i) = 1900 \text{ mg L}^{-1}$. Error bars represent standard deviation from three replicates.